Manuscript prepared for Hydrol. Earth Syst. Sci. Discuss.
with version 3.5 of the LaTeX class copernicus_discussions.cls.
Date: 27 June 2013

A simple lumped model to convert air temperature into surface water temperature in lakes

Sebastiano Piccolroaz, Marco Toffolon, and Bruno Majone

Department of Civil, Environmental and Mechanical Engineering, University of Trento, Italy

Correspondence to: Sebastiano Piccolroaz
(sebastiano.piccolroaz@ing.unitn.it)

Abstract

Water temperature in lakes is governed by a complex heat budget, ~~where the single fluxes are hardly assessable over long time periods in the absence of high accuracy data~~ where the estimation of the single fluxes requires the use of several hydro-meteorological variables that are not generally available . In order to address this issue, we developed Air2Water, a simple physically-based model to relate the temperature of the lake superficial layer (epilimnion) to air temperature only. The model has the form of an ordinary differential equation which accounts for the overall heat exchanges with the atmosphere and the deeper layer of the lake (hypolimnion) by means of simplified relationships, which contain a few parameters (from four to eight in the different proposed formulations) to be calibrated with the combined use of air and water temperature measurements. ~~In particular, the~~ The calibration of the parameters in a given case study allows ~~one~~ to estimate, in a synthetic way, the influence of the main processes controlling the lake thermal dynamics, and to recognize the atmospheric temperature as the main factor driving the evolution of the system. In fact, under certain hypotheses the air temperature variation implicitly contains proper information about the ~~variation of~~ other major processes involved, and hence in our approach is considered as the only input variable of the model. ~~Furthermore, the model~~ In particular, the model is suitable to be applied over long time scales (from monthly to interannual), and can be easily used to predict the response of a lake to climate change, since projected air temperatures are usually available by large-scale global circulation models. In this paper, the model is applied to Lake Superior (USA – Canada) considering a 27-yr record of measurements, among which 18 yr are used for calibration and the remaining 9 yr for model validation. The calibration of the model is obtained by using the Generalized Likelihood Uncertainty Estimation (GLUE) methodology, which also allows for a sensitivity analysis of the parameters. The results show a remarkable agreement with measurements, over the entire data period. The use of air temperature reconstructed by satellite imagery is also discussed.

1 Introduction

Water temperature is crucial for lakes physical, chemical and biological dynamics~~, indeed~~ : temperature is the primary driver of the vertical stratification, thus directly affects vertical exchanges of mass, energy and momentum within the water column. Water temperature plays a key role influencing the aquatic ecosystem of lakes, which usually adapts to a specific range of physical and environmental conditions. As a matter of fact, water temperature can affect both the chemical (e.g. dissolved oxygen concentration) and biological (e.g. fish growth) processes occurring in the water body (e.g. Wetzel, 2001). Recent studies demonstrate that lakes are highly sensitive to climate, and their physical, chemical, and biological properties respond rapidly to climate-related changes (Adrian et al., 2009). In the light of these considerations, it is evident that any significant modification to current environmental conditions may influence the limnic system, with direct impacts on the composition and richness of its ecosystem (MacKay et al., 2009). There are indeed several reasons to look for a reliable tool to have information about the dependence of water temperature on the various factors influencing the heat balance of the lake compartments.

~~Water temperature in lakes follows complex dynamics and is the result of a combination of different fluxes, whose sum is often small compared to the single terms. This is particularly true for the temperature of the well-mixed surface layer, usually termed as epilimnion during stratified conditions, which experiences strong oscillations at a variety of temporal scales: from short (a few days) to long (annual and interannual) up to climatic (decades to centuries).~~ Water temperature in lakes follows complex dynamics and is the result of a combination of different fluxes, whose sum is often small compared to the single terms (e.g. Imboden and Wüest, 1995). Therefore, relatively small errors in the estimate of the single contributions may result in a significantly large error in the evaluation of the net heat flux. This is particularly true for the well-mixed surface layer, usually termed as epilimnion during stratified conditions, which experiences strong oscillations at a variety of temporal scales: from short (hourly and daily) to long (annual and interannual) up to climatic (decades to centuries). Closing the heat balance correctly at the different scales and predicting the future trend of surface water temperature

Discussion Paper | Discussion Paper | Discussion Paper | Discussion Paper |

is therefore challenging, ~~but some difficulties are essentially harder to tackle.~~ and not always possible (e.g. if meteorological data are not sufficient). As a consequence, some hydrodynamic lake models prescribe surface water temperature as surface boundary condition instead of computing the net heat flux at the water-atmosphere interface (e.g. Goudsmit et al., 2002; Piccolroaz and Toffolon, 2013). In general, large uncertainties are associated to the estimates of the various heat exchange components; however the variables involved in the different processes are either not all independent from each other or do not present strong interannual variations, suggesting that some simplifications can be possibly adopted. ~~For instance, shortwave solar radiation substantially depends on the latitude of the lake, but has a rather regular annual trend~~ For instance, shortwave solar radiation substantially depends on the latitude of the lake and on cloudiness, with the former presenting a rather regular annual trend and the latter being important mainly at short time scales (from hourly to weekly) . Deep water temperature typically changes on time scales much longer than surface water, thus the heat exchanged with the hypolimnion can be reasonably assumed as constant in many situations. On the contrary, air temperature is a significant index of the overall meteorological conditions and can be reasonably assumed as the main variable influencing the heat balance of the surface layer of the lake (Livingstone and Padisák, 2007).

Thankfully, long-term, high-resolution air temperature observational datasets are in general available, both for historical periods adopted to calibrate General Circulation Models (GCMs) and Regional Climate Models (RCMs), and for future periods where air temperature is a variable commonly derived from GCMs or RCMs projections. ~~On the other hand water temperature measurements are far less available, and future projections are less reliable than modeled air temperature. The latter point is particularly true for climate change studies based on GCMs, whose mesh size is normally too coarse for explicitly including even some of the biggest lakes on Earth. These evidences explain why air temperature is typically used to derive surface temperature of water bodies.~~ On the contrary, water tempeature measurements are far less available and future projections could be only obtained through the adoption of predictive models fully coupled with atmospheric and land surface models, which at the present stage is not a common practice (MacKay et al., 2009). In order to overcome these limitations (i.e.

scarce availability and difficult estimation), several simple models have been formulated which use air temperature (widely accessible both for past and future periods) to derive surface water temperature of lakes.

Regression models (see Sharma et al., 2008, for a review) are typically adopted for this scope, but their use may be questionable especially when it is necessary to extrapolate temperature values beyond the maximum (or minimum) limit of the measured time series. This is often the case in climate change studies, where the regression relationships built upon current climate condition are applied to estimate surface water temperature for different climate change scenarios, with the possibility that the projected air temperature may cover a wider interval of values. Regression-type models, either linear or non-linear, have been successfully applied to estimate the temperature of rivers and streams, giving rise to a rich literature (e.g. Kothandaraman and Evans, 1972; Crisp and Howson, 1982; Webb et al., 2003; Benyahya et al., 2007; Morrill et al., 2005). Notwithstanding, ~~significant error may arise by adopting this approach~~ these models cannot straightforwardly be extended to the case of lakes , especially for those water basins that have a significant seasonal hysteresis. As a matter of fact, the variety of processes of heat exchange across the lake surface and the thermal inertia of the water mass cause an annual phase lag between air and water temperatures, which is hard to consider in regressions. In many cases simplistic linear regressions are adopted for the conversion, following the assumption of a direct monotonic relationship between air temperature and surface water temperature (e.g. Shuter et al., 1983; Livingstone and Lotter, 1998; Livingstone et al., 1999), which do not allow for capturing the hysteresis cycle. In other cases, seasonal hysteresis is solved by estimating different seasonal regression relationships, one for each branch of the hysteresis loop (e.g. one for the ascending and another for the descending branch) (e.g. Webb, 1974), or by using linear regressions to estimate the monthly means of surface water temperature from the monthly means of measured air temperature data (McCombie, 1959).

Besides regression analysis, water temperature of lakes can be estimated by means of process-based numerical models (e.g. Arhonditsis et al., 2004; Fang and Stefan, 1999; Peeters et al., 2002; Martynov et al., 2010), possibly coupled with an atmospheric model (e.g. Goyette and Perroud, 2012; Martynov et al., 2012) aimed at including the mutual interaction between water

and atmosphere. This kind of models can provide exhaustive information about the thermal structure of lakes, and accurately characterize the different energy fluxes involved in the lake temperature dynamics. The major drawback of the process-based models is the requirement of detailed time series of meteorological data in input (e.g. wind speed, humidity, cloudiness etc. besides air temperature), which are often not available or not accurate enough.

In order to overcome the limitations of traditional approaches (both regression- and process-based models), semi-empirical models based on physical principles may represent a valid alternative, having the key advantage of requiring less data in input than deterministic models, whilst preserving a clear physical basis. Recently, Kettle et al. (2004) proposed a simple empirical model to estimate mean daily water temperature, using only air temperature and the theoretical clear-sky solar radiation as input information. The model is based on the sensible heat exchange model of Rodhe (1952) (see also Bilello, 1964), and implicitly accounts for the main heat exchange processes through 4 parameters. The model has good performances, but its application is limited to specific periods of the year with nearly uniform stratification conditions (it has been tested from late June to early September, long after ice melts, when water temperature is always above 4 °C). ~~Indeed~~ However , it does not account for the seasonal evolution of the thermal structure of the lake, and hence of the mixing depth (i.e. the depth of the epilimnion), which determines the volume of water responding to ~~external~~ meteorological forcing and has a significant influence on the seasonal patterns of atmosphere-lake heat exchange.

In the attempt to reliably estimate the cycle of surface water temperature of lakes from air temperature measurements/projection only, both under past, current and projected climate conditions, a simplified model has been developed. Such a model is primarily based on the energy balance between atmosphere and lake surface water (Fig. 1), but avoids the need to take into account all heat budget terms explicitly. A simple parameterization of the seasonal evolution of the mixing depth is included in the model equations, which only depend upon air temperature. ~~This allows~~ The key objective of the present work is thus the definition of a modeling framework which could allow for a consistent description of the physical principles governing lake surface temperature, and ensures a general applicability of the model (e.g. over the entire year).

The paper is structured as follows. In Sect. 2 the governing equations are presented, and the model is formulated. The heat budget is presented in detail in Appendix A. Section 3 provides a general description of the data used in this study. The results concerning model calibration and validation are presented in Sect. 4 with reference to the different versions of the model and the various dataset used in this work. ~~Results are further discussed in Sect. 5, where the model is also tested using a different dataset (i.e. surface water temperature estimates from satellite imagery). Finally, the main conclusions are drawn in Sect. 6.~~ Results are discussed in Sect. 5, and finally we draw the main conclusions in Sect. 6.

2 Formulation of the model

The net heat flux H_{net} in the surface layer of a lake results from the combination of the different fluxes entering and exiting the upper water volume (see Fig. 1). The main heat exchanges occur at the interface between the epilimnion and atmosphere, and between the epilimnion and deep water (i.e. hypolimnion)~~, respectively~~. According to the simplifications discussed in Appendix A, a simplified version of the net heat flux can be expressed as

$$H_{\mathrm{net}} = c_1 \cos\left[\frac{2\pi\,(t - c_2)}{t_{\mathrm{y}}}\right] + c_3 + c_4\,(T_{\mathrm{a}} - T_{\mathrm{w}}) + c_5 T_{\mathrm{w}}, \tag{1}$$

where t is time, t_{y} is the duration of the year expressed in suitable time units, T_{a} and T_{w} are air and water temperature (expressed in Celsius [°C] for simplicity), respectively, and c_i (i from 1 to 5) are coefficients with a physical correspondence, whose definition is detailed in Appendix A. Note that Eq. (1) accounts for a sinusoidal annual forcing term with amplitude c_1 and phase c_2 (which result from a combination of the seasonal fluctuations of solar radiation and of sensible and latent heat fluxes), an exchange air-water term $c_4(T_{\mathrm{a}} - T_{\mathrm{w}})$ (where c_4 is a coefficient that is primarily ascribable to a transfer function of sensible heat flux), a constant term c_3 and a residual correction $c_5 T_{\mathrm{w}}$ dependent on the water temperature (the last two terms combined together basically account for the contribution of the latent heat flux). The only meteorological variable explicitly included in the model is T_{a}, while the remaining meteorological

Discussion Paper | Discussion Paper | Discussion Paper | Discussion Paper |

forcing (~~primarily wind, which is a major driving force for lakes~~ e.g. wind speed, solar radiation, humidity, cloudiness, which besides air temperature are the major factors controlling the heat budget of lakes) are inherently accounted for in the model's parameters. ~~The~~ In particular, the formulation of the model implicitly accounts for the seasonal patterns of these external forcing terms through the data-driven calibration of the parameters, while higher frequency fluctuations are not considered, consistently with the main aim of the model that is to reproduce the evolution of T_W at long time scales (i.e. ~~seasonal~~ monthly , annual, interannual).

Considering the upper layer of the lake, the volume-integrated heat equation can be expressed as follows

$$\rho c_p V \frac{\mathrm{d}T_\mathrm{W}}{\mathrm{d}t} = H_\mathrm{net} A, \tag{2}$$

where ρ is the water density, c_p is the specific heat at constant pressure, V and A are the volume and the surface area of the layer, respectively. Both V and A can be left undetermined in the analysis if we define the depth of the well-mixed surface layer (i.e. the epilimnion thickness) as follows

$$D = \frac{V}{A}. \tag{3}$$

The depth D typically depends on the stratification of the water column and is characterized by a clear seasonal behavior. In order to include this essential feature, a suitable parameterization of D in time is required. The most appropriate choice is to estimate D as a function of the thermal stratification, thus of the vertical temperature gradient. As a first approximation, the strength of the stratification can be evaluated as proportional to the difference between the surface water temperature T_W and a reference value T_r. T_r is representative of deep water temperature, thus can be suitably chosen depending on the thermal regime of the lake (for a classification of lakes refer to e.g. Hutchinson and Löffler, 1956; Lewis, 1983). In the case of cold monomictic lake (i.e. never over the temperature of maximum density $T_{\rho,\mathrm{max}} \approx 4\,^\circ\mathrm{C}$, stably stratified in winter and circulating in summer; in these lakes the thermal stratification is referred to as inverse since water temperature at the surface, T_W, is colder than in the hypolimnion) T_r can be assumed as the maximum surface temperature registered during the year.

In the case of warm monomictic lakes (i.e. always above 4°C, circulating in winter and stably stratified in summer; in these lakes the thermal stratification is referred to as direct since water temperature at the surface, T_{w}, is warmer than in the hypolimnion) T_{r} can be assumed as the minimum surface temperature registered during the year. Finally T_{r} can be assumed equal to the temperature of maximum density $T_{\rho,\mathrm{max}} \approx 4\,^{\circ}\mathrm{C}$ for the case of dimictic lakes (i.e. inversely stratified in winter, stably stratified in summer and circulating twice a year at the transition between the two states, at about 4 °C). In all cases, when the water column is nearly isothermal (i.e. $T_{\mathrm{w}} \rightarrow T_{\mathrm{r}}$), close to the onset of the seasonal turnover, the thermal stratification weakens and, as a consequence, the surface mixed layer D reaches its maximum thickness D_{r}. On the contrary, we assume that the stronger is the stratification (i.e. $|T_{\mathrm{w}} - T_{\mathrm{r}}| \gg 0$), the thinner is the surface mixed layer D.

For the period of direct stratification ($T_{\mathrm{w}} > T_{\mathrm{r}}$), the evolution of D ~~has been~~ is described using the simple exponential decay law

$$D(t) = D_{\mathrm{r}} \exp\left(-\frac{T_{\mathrm{w}}(t) - T_{\mathrm{r}}}{\tau_{\mathrm{warm}}}\right), \tag{4}$$

where τ_{warm} [°C] is the inverse of the decay rate (the subscript $warm$ refers to the case $T_{\mathrm{w}} > T_{\mathrm{r}}$: direct stratification) and D_r indicates the maximum thickness of the mixed layer. With the aim to consider the variation of D when the lake is inversely stratified (i.e. $T_{\mathrm{w}} < T_{\mathrm{r}}$, subscript cold), a modified version of Eq. (4) has been derived,

$$D(t) = D_{\mathrm{r}} \left[\exp\left(-\frac{T_{\mathrm{r}} - T_{\mathrm{w}}(t)}{\tau_{\mathrm{cold}}}\right) + \exp\left(-\frac{T_{\mathrm{w}}(t) - 0°\mathrm{C}}{\tau_{\mathrm{ice}}}\right)\right], \tag{5}$$

where τ_{cold} [°C] and τ_{ice} [°C] are the inverse of decay rates. In principle, τ_{cold} is not necessarily equal to τ_{warm}, since the evolution of D below and above T_{r} is possibly different. In addition, the second term in the exponential function has been introduced to account for the potential formation of the ice cover at the surface. ~~In this case, as T_{w} tends to 0 °C, D thickens, and in our scheme this indirectly takes into account the inhibition of the air-water heat flux due to the presence of ice and snow covers.~~ As T_{w} tends to 0 °C, the air-water heat flux is inhibited due to the presence of ice and snow covers. Our scheme indirectly takes this into account by a

fictitious increase of the depth D. It is worth ~~to notice~~ noting that τ_{ice} should have an upper bound (approximately equal to 0.5 °C ~~in our case~~), in order to include the effect of ice only when the lake is inversely stratified, and avoid a discontinuity in D at the transition from direct to inverse stratification (i.e. when $T_{\mathrm{w}} = 4\,^{\circ}\mathrm{C}$).

By substituting Eqs. (1), (3), (4) and (5) into Eq. (2) we obtain

$$\frac{\mathrm{d}T_{\mathrm{w}}}{\mathrm{d}t} = \frac{1}{\delta}\left\{p_1 \cos\left[\frac{2\pi\,(t-p_2)}{t_{\mathrm{y}}}\right] + p_3 + p_4\,(T_{\mathrm{a}} - T_{\mathrm{w}}) + p_5 T_{\mathrm{w}}\right\}, \tag{6}$$

with

$$\begin{aligned}
\delta &= \exp\left(\frac{T_{\mathrm{r}} - T_{\mathrm{w}}}{p_6}\right), \quad (T_{\mathrm{w}} \geq T_{\mathrm{r}}) \\
\delta &= \exp\left(\frac{T_{\mathrm{w}} - T_{\mathrm{r}}}{p_7}\right) + \exp\left(-\frac{T_{\mathrm{w}}}{p_8}\right), \quad (T_{\mathrm{w}} < T_{\mathrm{r}})
\end{aligned} \tag{7}$$

where the model parameters p_i ($i = 1, 3, 4, 5$) are the coefficients c_i present in Eq. (1) divided by the product $\rho c_{\mathrm{p}} D_{\mathrm{r}}$, $p_2 = c_2$, $p_6 = \tau_{\mathrm{warm}}$, $p_7 = \tau_{\mathrm{cold}}$, $p_8 = \tau_{\mathrm{ice}}$, and $\delta = D/D_{\mathrm{r}}$ is the normalized depth, whose seasonal evolution is schematically represented in Fig. 2 for the case of dimictic lakes (monomictic regimes are particular cases of the dimictic regime, which represents the most general case).

In conclusion, we propose a semi-empirical lumped model, which solves the temporal evolution of surface water temperature of lakes, using only air temperature as input forcing. The model requires the calibration of 8 physically-based parameters, whose range of variation can be reasonably estimated according to their definitions (see Appendix A).

3 Study site

In order to apply the model described in Sect. 2, only two series of data are required: air temperature as input forcing, and surface water temperature for calibration purpose. A sufficiently long dataset (i.e. more than one year) is an essential prerequisite to perform a robust model

calibration and validation procedure. Moreover, a long-term dataset provides a clear picture of the possible interannual temperature variability, thus allowing for the identification of a set of parameters that is appropriate to investigate long-term climate dynamics.

The model has been tested on Lake Superior (Surface area: 82 103 km^2; Volume: 12 000 km^3; Maximum depth: 406 m), the largest of the five Great Lakes of North America (see Fig. 3), and the largest freshwater basin in the world by surface area. Lake Superior is a dimictic lake: the temperature of the epilimnion is warmer than 4 °C in summer and cools below 4 °C in winter. While the surface water temperature varies seasonally, the temperature of the hypolimnion is almost constant over the year at about 4 °C. Twice a year, in December and in June, surface water reaches ~~the temperature of 4 °C~~ this temperature , thus the thermal stratification weakens. Under these conditions, and in the presence of a sufficiently strong wind blowing at the surface, the entire lake can mix (i.e. lake's turnover).

Long-term temperature data (both for air and surface water) have been obtained from the National Data Buoy Center (NDBC) and from the Great Lakes Environmental Research Laboratory (GLERL), which are part of the National Oceanic and Atmospheric Administration (NOAA). In particular, the NDBC provides historical meteorological and oceanographic data for a network of offshore buoys and Coastal Marine Automated Network (C-MAN) which are installed all over the world, while the GLERL, through the CoastWatch program, releases daily digital maps of the Great Lakes surface water temperature and ice cover (i.e. the Great Lakes Surface Environmental Analysis – GLSEA). ~~For the purpose of this work, only air and surface water temperatures are required, thus other variables are not presented here.~~

Concerning NDBC dataset, two different stations have been used in this work: (a) 45004 – Marquette, an offshore mooring buoy that provides water temperature measured at 1 m below the water surface, and (b) STDM4 – Stannard Rock, a C-MAN station installed on a lighthouse that provides air temperature series measured at about 35 m above the lake surface. These two stations have been chosen from the many that are available for Lake Superior (both offshore buoys and C-MAN), because of their central location (see Fig. 3) and long-term data availability, but time series registered in other stations present similar behavior (not presented here). The observational dataset cover a 27-yr long period, from 1985 to 2011, and consists of mea-

surements with ~~a~~ one-hour temporal resolution. Since NDBC buoys in the Great Lakes are removed during winter to prevent damage from icing, no measurements are available at the 45004 – Marquette during winter months (except for 1991), while the STDM4 – Stannard Rock measurements do not show ~~significant~~ systematic gaps.

~~Concerning GLERL dataset, daily temperature maps have been used for the period 1994 to 2011. Data refer to the daily lake average surface water temperature obtained from NOAA polar-orbiting satellite imagery. The series is almost continuous, and does not present significant gaps. Schwab et al. (1999) compared GLERL surface water temperatures estimates with water temperatures measured at some of the NDBC buoys, finding an overall good agreement, with a mean difference between the two of less than 0.5 °C and a root mean square differences ranging from 1.10 to 1.76 °C. The close correspondence between the two sets of data is confirmed in Fig. 8a where NDBC and GLERL dataset considered in the present study are compared for the period 2003–2011.~~ Concerning GLERL dataset, daily temperature maps have been used for the period 1994 to 2011. Data refer to the daily lake average surface water temperature obtained from NOAA polar-orbiting satellite imagery. The series does not present systematic gaps (missing data, see Table 1, are concentrated in the first, warm-up year and hence do not contribute to the evaluation of the model efficiency, see Sect. 4.1), thus providing surface water temperature also in winter, which, on the contrary, is almost completely uncovered by the NDBC dataset. A mismatch between NDBC and GLERL datasets is visible in the rising limb of the annual cycle of temperature (i.e. between April and July, see Fig. 8a), which is likely to be a consequence of the different spatial scales of the two series of data: while the NDBC dataset represents surface water temperature measured nearly at the center of the basin, the GLERL dataset provides values averaged over the whole lake. In the latter case, the spatial variability of surface water temperature (e.g. in spring, lake water heats from the shores towards the offshore deeper zones) is intrinsically included in the estimates, thus determining smoother annual cycles of temperature. Despite this discrepancy, Schwab et al. (1999) compared GLERL data with measurements at some of the NDBC buoys finding an overall good agreement. In particular, for the case of the 45004 - Marquette buoy used in this work, the mean difference between the two datasets for the period 1992 - 1997 is less than $0.28°C$, the root mean square

error is $1.10°C$ and the correlation coefficient is 0.96.

As customary, the available datasets have been divided into two parts: the first part, containing around two thirds of the available data, is used for model calibration and sensitivity analysis, while the second part, containing the remaining one third, is used for model validation. Missing data in the water temperature series have not been replaced (they do not contribute to the evaluation of the efficiency of the model); on the other hand, gaps in the air temperature series have been reconstructed with estimates obtained as an average of the available data in the same day over the corresponding period (i.e. calibration or validation). The datasets used in this work are listed in Table 1, together with their main statistics.

~~The differential Eq. (6) has been solved numerically by using the Euler explicit numerical scheme, with a daily time step (concerning NDBC data, mean daily temperatures have been preliminary calculated from the original data).~~ The differential Eq. (6) has been solved numerically by using the Euler explicit numerical scheme (see e.g. Butcher, 2003) , with a daily time step (concerning NDBC data, mean daily temperatures have been preliminary calculated from the original data).

4 Results

4.1 Sensitivity analysis and model calibration

Inverse modeling of complex systems, as such as those encountered in hydrological applications, is inherently ill posed problem, as the information provided by observational data is insufficient to identify the parameters without uncertainty. In a typical situation many different combinations of the parameters may provide similar fitting to the observational data. For example, even a simple model with only four or five parameters to be estimated may require at least ten hydrographs for a robust calibration (e.g. Hornberger et al., 1985).

This identification problem can be alleviated by reducing the number of parameters used in the model, for example through sensitivity analysis, which is the typical methodology used for this purpose (e.g. Majone et al., 2010). In this work we perform sensitivity analysis by using

Generalized Likelihood Uncertainty Estimation (GLUE), a methodology proposed by Beven and Binley (1992) that requires the identification of a validity range for each parameter, a strategy for sampling the parameter space and finally a likelihood measure to be used in order to rank the different parameters sets. We carried out 100 000 000 Monte Carlo model realizations using uniform random sampling across specified parameter ranges selected according to physical limitations of model's parameters. Indeed, the physical meaning of the parameters allowed for a reasonable definition of the possible range of variability of each of them. Finally, we used as likelihood measure the Nash-Sutcliffe model efficiency coefficient, E, which is a widely used metric adopted in hydrological applications (e.g. Nash and Sutcliffe, 1970; Majone et al., 2012, and many others)

$$E = 1 - \frac{\sigma_e^2}{\sigma_o^2} = 1 - \frac{\sum_{i=1}^{n} \left(\widehat{T}_{\mathrm{W},i} - T_{\mathrm{W},i} \right)^2}{\sum_{i=1}^{n} \left(\widehat{T}_{\mathrm{W},i} - \overline{T}_{\mathrm{W},i} \right)^2}, \tag{8}$$

where n is the number of data, σ_e^2 and σ_o^2 are the variance of the residuals and of the observations, respectively, $\widehat{T}_{\mathrm{W},i}$ and T_{W} are the observed and simulated surface water temperature at time t_i, and $\overline{T}_{\mathrm{W}}$ is the average of $\widehat{T}_{\mathrm{W},i}$. Note that the residual is defined as the difference between the observational data and the model's prediction, and a parameter set identifies a point in the space of parameters.

The Nash-Sutcliffe efficiency index ranges from $-\infty$ to 1. An efficiency equal to 1 ($E = 1$) corresponds to a perfect match between measured and simulated values, whilst $E = 0$ indicates that the model prediction is as accurate as the mean of observations. Efficiency values lower than 0 ($E < 0$) occurs when σ_e^2 is larger than σ_o^2, thus when the mean of observations is a better estimator than the model itself.

Since its introduction in 1992, GLUE has found wide applications and it is recognized as a useful methodology for uncertainty assessment in many fields of study especially in non-ideal situations (e.g. Beven, 2006). Nevertheless, the goal of this work is not to adopt a complete informal Bayesian approach to estimate uncertainty of model predictions, but rather to assess

the impact of changes in uncertain parameter values on model output. Hence, the purpose is to set up a general and effective strategy to select which are the most sensitive parameters of the model, and to define which should be suitably adjusted in a calibration process. Indeed, the GLUE methodology is a powerful and effective tool that can be also used for model calibration besides uncertainty estimation procedures and sensitivity analysis.

One of the most acknowledged limitation of the GLUE methodology is the dependence on the number of Monte Carlo simulation, especially in the presence of complex models with high computational demand. However, in our case we were able to fully explore parameter response surfaces by adopting a significantly high number of realizations. Therefore, the use of the GLUE methodology, not only for parameter identifiability purposes but also as a calibration tool, appears appropriate. Just as a sidenote, 100 000 000 model runs over a period of 18 yr with a daily time step and adopting Intel(R) Xeon(R) CPU X5680 @ 3.33 GHz took around 2 h; the code is written in Fortran 90.

Furthermore, in the attempt to test reliability and predictive capability of the model, a validation procedure was undertaken by running the model on validation datasets (see Table 1) by using the sets of parameters which maximize the efficiency E during the calibration periods (i.e. the set of parameters with the highest likelihood obtained through the GLUE methodology).

In the ensuing sections, the GLUE methodology is presented for different model configurations (from 8 to 4 parameters), with reference to the calibration periods of the NDBC and GLERL datasets, respectively (see Table 1).

As a final comment, we point out that the first year of each time series is used as warm-up period (i.e. excluding the period from the calculation of the Nash–Sutcliffe efficiency index E), in order to remove any transient effect due to the initial condition.

4.2 8-parameter model

As discussed in the previous section, the performance of the model has been tested in the framework of the GLUE methodology, using the time series of air and surface water temperatures provided by the NDBC center (see Table 1). A first-step sensitivity analysis has been carried out by solving Eq. (6) over the calibration period (18 yr, from 1985 to 2002) using

randomly sampled set of parameters. We recall here that each of the 8 parameters has been allowed to vary over physically reasonable ranges of values, which have been previously determined through Eqs. (A12)–(A16) in Appendix A by considering the lake location properties (e.g. latitude, climate, typical temperatures) and by using coefficients available in literature (e.g. Henderson-Sellers, 1986; Imboden and Wüest, 1995; Martin and McCutcheon, 1998). As far as the exponential decay laws are concerned, parameters p_6 and p_7 have been allowed to range within a wide interval comprised between 0 and 15 °C, and p_8 between 0 and 0.5 °C. As already mentioned in Sect. 2, the range of p_8 has been set narrower (more stringent upper bound), aimed at confining the correction due to ice only when the lake is inversely stratified ($e^{-4/0.5} = \mathcal{O}(10^{-4}) \ll 1$). In the light of the results obtained from the first-step analysis, the ranges of variability of each parameter were narrowed, thus allowing for a detailed investigation of parameters space regions associated with high values of E. Subsequently, a second-step sensitivity analysis has been undertaken by sampling further 100 000 000 parameters sets from the narrowed parameters ranges.

Figure 4 shows the dotty plots of the efficiency index E for each of the 8 parameters of the model, corresponding to the narrowed ranges (second-step performance analysis). For the sake of clarity in the presentation of results, Fig. 4 (as well as Fig. 6) shows only the set of parameters with E larger than 0.8. Model simulation during the calibration period 1985–2002 using the best set of parameters is illustrated in Fig. 5, which shows a noticeable agreement between simulated and observed values, with an efficiency index $E > 0.9$ (see ~~Table 2~~ Tables 2 and 3 for a summary of the results).

A visual inspection of dotty plots of model efficiency can provide useful information on the identifiability of each parameter. According to Fig. 4, all the parameters are characterized by a good identifiability with the exception of parameters p_7 and p_8. This can be explained if we consider that NDBC dataset presents only a few values of water temperature during winter periods. In particular, no data (except for one single year out of 18) are available when surface water temperature approaches 0 °C, which corresponds to the period of the year when the parameter p_8 is relevant. We remark here that p_8 is the parameter associated to ice formation at the surface of the lake. Although to a minor extent, also p_7 does not show a clear identifiability, probably as

a consequence of the importance that this parameter assumes only during winter time (it plays a role only when $T_W < 4\,°C$), that is when water temperature measurements are not available. However, by analyzing the dotty plot an important information can be inferred: efficiency increases for higher values of p_7, and approaches a nearly asymptotic high efficiency trend when $p_7 \gtrsim 5\,°C$. Looking at the physical meaning of the parameter (see Eq. 7), this means that model performance improves as the mixed depth D approaches its maximum value D_r when the lake is inversely stratified ($T_W < 4\,°C$).

~~On~~ In the light of these evidences, in the ensuing section the full 8-parameter version of the model has been simplified by neglecting parameters p_7 and p_8.

4.3 From 8 to 4 parameters

On the basis of the results discussed in the previous section, not all the model parameters seem to be significant and clearly identifiable. In particular, the parameter p_8 has been found to be insensitive to the model, and parameter p_7 provides an overall high performance over most of its variability domain ($p_7 \gtrsim 5\,°C$). The peculiar behavior of these parameters, together with the fact that both appear in the definition of the mixing depth D when the lake is inversely stratified, suggests that a simplification of the model may be possible by considering a different (simpler) expression for D. As far as parameter p_8 is concerned, since it is not significant for the model, it can be easily neglected, thus eliminating the effect of ice formation. On the other hand, according to Eq. (7) high values of p_7 mean small decay rates of D, thus thick mixing depths when the lake is inversely stratified. In the light of these considerations, we derived a first simplified version of the model, where the mixing depth is assumed to be constant and at its maximum thickness $D = D_r$ when the lake is inversely stratified ($T_W < T_r$). Thanks to this simplification p_7 and p_8 are removed and the number of parameters diminishes from 8 to 6.

As for the case of the full 8-parameter version of the model, the same sensitivity analysis described in Sect. 4.2 has been carried out also for the simplified 6-parameter version. The set of parameters presenting the highest efficiency index during the calibration period is summarized in Table 2, whilst dotty plots deriving from the application of GLUE methodology and the comparison between simulated and measured surface water temperature during the same period

are not presented here for the sake of brevity. Indeed, results are essentially equivalent to those obtained using the full 8-parameter model, which is confirmed by the close similarity between the best set of parameters and the efficiency indexes obtained in the two cases (see ~~Table 2~~ Tables 2 and 3). The similarity of results supports the idea that the 6-parameter model is a reasonable simplification, at least in the case considered herein where the winter data are not abundant (see also Sect. 5 for further discussion).

The number of parameters can be further diminished from 6 to 4 by eliminating the parameter p_1 and, as a direct consequence, p_2, besides p_7 and p_8. This simplification is justified since three periodic terms appear in the model as characterized by an annual periodicity: the forcing term $p_1 \cos(2\pi(t - p_2))$, the exchange term $p_4(T_\mathrm{a} - T_\mathrm{w}$ and the residual correction $p_5 T_\mathrm{w}$. The simultaneous co-presence of all these terms may be considered redundant in those cases in which the annual cycles of T_w and/or of $T_\mathrm{a} - T_\mathrm{w}$ can be suitably approximated as sinusoids. Indeed, the sum of sinusoidal functions with the same frequency, but different amplitude and phase, yields ~~to~~ another sinusoid with different amplitude and phase but same frequency. Therefore, two sinusoids are sufficient, and the forcing term $p_1 \cos(2\pi(t - p_2))$ can be removed, relieving the overall annual variations on the periodic terms controlled by the model variable T_w and the external forcing T_a. Following this logic, the term $p_5 T_\mathrm{w}$ could be neglected alternatively (on the contrary $p_4(T_\mathrm{a} - T_\mathrm{w})$ cannot since it is the only term that includes information about the external forcing), but this assumption would remove only one parameter (p_5) instead of two (p_1 and p_2), thus making it less attractive. In principle, both $p_1 \cos(2\pi(t - p_2))$ and $p_5 T_\mathrm{w}$ could be neglected contemporaneously, but in this case the phase of the overall periodic term would be forced to that of the temperature difference. It is worth ~~to note~~ noting that in the 4-parameter version of the model (retaining p_3, p_4, p_5 and p_6), the meaning of the parameters is distorted, as the processes that were accounted in p_1 are now included in p_4 and p_5.

Figure 6 shows the dotty plots of the efficiency indexes E for the 4-parameter version of the model, where only the parameters p_3, p_4, p_5 and p_6 are retained. In this case, since the number of random samplings has been kept unchanged (i.e. 100 000 000), the predictions of the Monte Carlo realisations appear much less sparse (i.e. denser dotty plots) if compared to the case of the 8-parameter version. Notice that all the parameters are characterized by high identifiability

and the model does not present signs of overparameterization. Figure 5 shows the comparison between observed and simulated surface water temperatures during the calibration period 1985–2002 for the 4-parameter and the full 8-parameter models, respectively. The difference is ~~little,~~ small, and mainly localized during the winter period, when no surface water temperature data are available for comparison. During the rest of the year, when measurements are available and E index can be effectively calculated, the two solutions are comparable and the efficiency indexes are similar (just slightly lower for the simplified 4-parameter version of the model, see Table 2).

4.4 Model validation

The best set of parameters obtained during the calibration period for the different versions of the model (with 8, 6 and 4 parameters, see Table 2) have been used to run the model during the validation period 2003–2011 (see Table 1). In all the cases, simulations have been characterized by high efficiency indexes, comparable to those obtained with the best simulations during the calibration period ($E \simeq 0.9$, see Table 2). In Fig. 7 simulated water temperatures (for the versions with the 8 and 4 parameters) are compared with observations showing an overall very good agreement. Results confirm the reliability of the model as a valuable tool for surface water estimation over long-term periods with different model configurations.

Besides the evaluation of the surface water temperature, the model provides additional ~~relevant~~ qualitative information regarding the annual evolution of the epilimnion thickness. In fact, as discussed in Sect. 2, the model explicitly includes a suitable parameterization of the seasonal behavior of the mixing depth through Eq. (7). In particular, the normalized thickness of the epilimnion $\delta = D/D_\mathrm{r}$ is automatically determined once the parameters p_6, p_7 and p_8 are defined. Furthermore, it is evident that if an estimate of the reference mixing depth D_r were known, the actual thickness of the well-mixed layer D could be evaluated as well. With reference to the NDBC dataset Fig. 8b shows the evolution of δ over the validation period 2003–2011, for the 8- and 4-parameter versions of the model (continuous lines). In the first case (8 parameters) the fictitious increase of depth due to the presence of ice is evident (peaks at values greater than 1). ~~We recall here that in the 8-parameter version of the model, the formation of ice is modeled by~~

~~increasing the depth D of the surface layer, thus the volume of water involved~~ Such an increase is related to the presence of a larger water volume involved in the heat balance (see Fig. 2). Thanks to this assumption the model accounts for the insulation effect due to the presence of ice, which may be even more significant when the ice surface is snow-covered, and the penetration of solar radiation is strongly attenuated.

4.5 Satellite data

Results are remarkable both using the full 8-parameter version and the simplified 6- and 4-parameter versions of the model. In particular, little difference has been found regarding the best set of parameters and the efficiency indexes obtained using the 8- and the 6-parameter versions (see Tables 2 and 3). Therefore, one may infer that no significant advantages can be expected by using a more accurate expression for D during the winter period (8-parameter version), instead of a constant value (6-parameter version). However, it is not possible to state this conclusion by simply analyzing results presented in Sects. 4.2, 4.3 and 4.4. Indeed, no surface water temperature measurements are available during the winter period for the NDBC dataset, except for the year 1991, thus the model efficiency has not been tested during the period of inverse stratification.

Aimed at overcoming this limitation, the GLERL dataset has been used, which provides daily lake-averaged surface water temperature based on satellite imagery and covers the whole year (see Table 1). The same GLUE procedure discussed in Sect. 4.1 has been performed by adopting the GLERL dataset as reference surface water temperature data and by repeating the implementation details described in Sect. 4.2. The simulations (hereafter referred to as GLERL) have been run over the calibration period 1994-2005, using as input forcing the air temperature data retrieved from the NDBC dataset (C-MAN station, see Table 1). The 8-, 6- and 4-parameter versions of the model have been tested, obtaining remarkable efficiency indexes ($E > 0.95$), which are higher with respect to the previous applications (i.e. using NDBC dataset). Validation procedure has been conducted with reference to the period 2006-2011, confirming high performances of the model ($E > 0.97$). The parameters sets providing the highest efficiencies during the calibration period and the associated E values are given in

Tables 2 and 3, while comparison between simulated and observed surface water temperature data for the 8- and 4-parameter versions of the model are shown in Figs. 9 and 10 for the calibration and validation periods, respectively. Finally, the seasonal evolution of δ is shown in Fig. 8b for both versions of the model (dashed lines), and it is compared with those obtained from the application of the model to the NDBC dataset. Results are consistent, with the slight difference in the onset of summer stratification being due to the earlier increase of water temperature in the GLERL dataset compared to the NDBC dataset (see Fig. 8a).

5 Discussion

The physically-based, semi-empirical model presented here has been shown to provide an accurate description of surface water temperature of lakes, with high values of Nash-Sutcliffe efficiency index $E \simeq$ ~~0.90,~~ 0.9, and a root-mean-square error between observations and simulations of the order of 1 °C (~~results not presented here~~ see Table 3). This error in prediction capability is comparable to those obtainable using process-based numerical models (e.g. Fang and Stefan, 1996; Stefan et al., 1998)~~. However, these kinds of models have the strong limitation of requiring high resolution weather data.~~ which however have the strong limitation of requiring high resolution weather data and the calibration of numerous internal parameters.

The close agreement between measurements and model estimates is further confirmed in Figs. 11a and 11b, which illustrate the parity diagrams for monthly-averaged surface water temperature during the calibration and validation periods of GLERL simulation, respectively. No systematic deviation (bias) is observed and the dispersion along the diagonal does not exhibit significant trends. Both these characteristics are confirmed by the small values of Mean Error (ME) and Root Mean Square Error ($RMSE$) listed in Table 3. Figures 11a and 11b also illustrate that the model is able to adequately describe interannual fluctuations, as is indicated by the range of variability of monthly-averaged temperatures associated to the coldest (March, blue dots) and warmest (August, red dots) months. This evidence is also confirmed by Figs. 9 and 10, where the model coherently reproduces the occurrence of relatively colder (e.g. 2004) and warmer (e.g. 1998) periods.

Results are remarkable both using the full 8-parameter version and the simplified 6- and 4-parameter versions of the model. In particular, little difference has been found regarding the best set of parameters and the efficiency indexes obtained using the 8- and the 6-parameter versions (see Table 2). Therefore, one may infer that no significant advantages can be expected by using a more accurate expression for D during the winter period (8-parameter version), instead of a constant value (6-parameter version). However, it is not possible to state this conclusion by simply analyzing results presented in Sects. 4.2, 4.3 and 4.4. Indeed, no surface water temperature measurements are available during the winter period for the NDBC dataset, except for the year 1991, thus the model efficiency has not been tested during the period of inverse stratification. Aimed at overcoming this limitation, a new dataset of surface water temperature has been used, which does not have significant data gaps: the daily lake-averaged surface water temperature based on satellite imagery provided by the GLERL (see Table 1). The same GLUE procedure discussed in Sect. 4.1 has been performed by adopting the GLERL dataset as reference surface water temperature data and by repeating the implementation details described in Sect. 4.2. The simulations (hereafter referred to as GLERL) have been run over the calibration period 1994-2005, using as input forcing the air temperature data retrieved from the NDBC dataset (C-MAN station, see Table 1). The 8-, 6- and 4-parameter versions of the model have been tested, obtaining remarkable efficiency indexes ($E > 0.95$), which are higher with respect to the previous applications (i.e. using NDBC dataset). Validation procedure has been conducted with reference to the period 2006–2011, confirming high performances of the model ($E > 0.97$). The parameters sets providing the highest efficiencies during the calibration period and the associated E values are given in Table 2, while comparison between simulated and observed surface water temperature data for the 8- and 4-parameter versions of the model are shown in Figs. 9 and 10 for the calibration and validation periods, respectively. Finally, the seasonal evolution of δ is shown in Fig. 8b for both versions of the model (dashed lines), and it is compared with those obtained from the application of the model to the NDBC dataset. Results are consistent, with the slight difference in the onset of summer stratification being due to the earlier increase of water temperature in the GLERL dataset compared to the NDBC dataset (see Fig. 8a).

So far, the model has been tested with long-term series of data (NDBC: 27 yr, and GLERL: 18 yr), ~~anyway~~ however long-term records are often not available, or are characterized by significant gaps due to missing data. Instead, it is relatively easier to have access to mean annual cycles of temperature (both of surface water and air), whose determination also represents a valuable strategy to overcome the possible lack of data. Therefore, a conversion model that could be calibrated on mean annual cycles, and successively applied over long-term periods without compromising the correct estimation of the interannual fluctuations, would represent a valuable tool. For this purpose, the mean annual cycle of surface water temperature has been derived from GLERL data during the calibration period 1994–2005, and the corresponding cycle of air temperature from NDBC dataset (C-MAN station). A Monte Carlo sensitivity analysis (hereafter referred to as $\mathrm{GLERL_{my}}$, the subscript $_{\mathrm{my}}$ staying for mean year) has been carried out following the same procedure adopted in the previous sections, but using mean annual cycles of air and water temperature as forcing and reference data, respectively. In order to eliminate the influence of initial conditions the temperature cycles have been replicated for two years with the first one used as a "warm-up". Results obtained by adopting the parameters providing the highest efficiency (see Table 2) are presented in Fig. 12, which shows the hysteresis cycles between air and surface water temperatures derived from measurements and model estimates (8- and 4-parameter versions). A very high efficiency index ($E \simeq 1.0$) is achieved, and both versions of the model are able to satisfactorily capture the seasonal pattern of thermal hysteresis. Parameters set providing the highest efficiency during the calibration process with the mean annual temperature data and the associated E value are summarized in ~~Table 2.~~ Tables 2 and 3.

Afterwards, a validation procedure has been conducted for $\mathrm{GLERL_{my}}$ during the period 2006–2011 (the same as GLERL simulations, thus results can be compared). Results are characterized by remarkable efficiency indexes ($E \simeq 0.97$), only slightly lower than the values obtained with the simulations presented in the previous sections. Indeed, the model calibrated on the mean year is able to well capture the interannual variabilities, producing remarkable results not dissimilar from those shown in Fig. 10 (for this reason they are not presented here). Furthermore, parameters values are significantly similar to those obtained calibrating the model with

the whole 12-yr series of data (GLERL simulation, see Table 2).

~~On~~ In the light of the results presented in this section, we assert that the model can be calibrated and adopted using data of different origin (measurements at buoys and coastal stations, satellite estimates) and nature (long-term series of data, mean annual cycle of temperature). This conclusion is corroborated by the excellent results (not shown here for the sake of brevity) of the performance analysis (entirely comparable to those presented in the present paper) obtained using different datasets: (a) air temperature from a different C-MAN station (the PILM4 – Passage Island), whose sensor is installed at a different high (22 m) respect to the Stannard Rock station (35 m), (b) air temperature data measured at the 45004 – Marquette offshore buoy station at only 4 m from the lake surface, and (c) water temperature measured at a different off shore buoy (the 45001 – Hancock). Furthermore, in all cases, even if the calibration is performed considering mean annual cycles of temperature, the model suitably captures the interannual variations that are likely to occur. On the basis of ~~these evidences~~ this evidence , we can assert that ~~in principles~~ this simple model may be used with different air temperature datasets ~~in~~ as input~~. As a matter of fact,~~ and, unlike process-based models, it can be calibrated using any water temperature dataset, independently of its physical representativeness (e.g. point measurements vs. spatial averages). ~~Air~~ Therefore, in principle, air temperature series provided by ~~general atmospheric models or climate projections derived from~~ GCMs and RCMs can be used as well. In this regard, the model is particularly attractive for climate change impact studies, since predictions of air temperature are usually more reliable and available than other meteorological variables (e.g. Gleckler et al., 2008). Based upon these considerations, Piccolroaz (2013) exploited the same approach to reproduce the current status and to predict future modifications of surface water temperature of Lake Baikal (Siberia).

6 Conclusions

In this work a simple, physically-based model has been developed to estimate surface water temperature from air temperature. In particular, we show that our modeling framework is able to reproduce the observed water temperature data with limited information on external meteo-

rological forcing over long time scales, ranging from monthly to interannual.

Starting from the zero-dimensional heat budget, we derived a simplified first-order differential equation for water temperature forced by a few terms representing the combined effects of the seasonally varying external ~~term~~ terms and the exchange terms explicitly dependent on the difference between air and water temperatures. Assuming annual sinusoidal cycles of the main heat flux components, 8 parameters have been identified, which can be calibrated if temporal series of air and surface water temperature are available. Such a calibration is supported by the physical interpretation of the parameters, which provides reasonable initial conditions for the parameters ranges.

The relative importance of the model's parameters have been evaluated by using the GLUE methodology. Thanks to this analysis we were able to identify and neglect parameters that, under different conditions, appears less significant in the model formulation leading to two simplified versions retaining 6 and 4 parameters, respectively.

The model has been applied to the case of Lake Superior (USA – Canada) with reference to different types of datasets, and all the versions of the model have shown to perform well in reproducing the measured water temperature data. This model has proved to be robust and able to ~~reproduce well~~ suitably simulate the lake's response to meteorological forcing, including ~~inter-annaul~~ interannual variability, representation of the variability of the epilimnion thickness, and the inverse startification process which typically occurs in dimictic lakes. In our view, Air2Water represents a valuable alternative tool to correlation models, which require the same data in input as our model but are not able to address some fundamental processes (e.g. the hysteresis cycle between air and water temperature). Furthermore it can be used in place of full process-based models when meteorological data are not sufficient for their effective application. In principle, the simple model presented here is likely to be effectively applied to lakes with different characteristics, although some inconsistencies could arise in those cases where the assumptions on which the model formulation has been based (see Appendix A) are no longer valid (e.g. tropical lakes characterized by intense evaporation, basins in which the through-flow is consistent, lakes located in regions where the variability of meteorological forcing is significant at sub-annual frequency).

In the light of ~~the~~ these results, the model can represent a valuable tool in climate change impact studies allowing for predictions of future trends of lake surface water temperature, given future projections of air temperature only. Finally, it is worth noting that if the model is calibrated using air temperature series from climate models (global or regional scale) and measured records of water temperature (lake scale), a downscaling operation is implicitly implemented in the conversion procedure (Piccolroaz, 2013).

Appendix A Simplified heat fluxes

Indicating with H the generic heat flux per unit surface [W m^{-2}], defined as positive when it is directed towards the considered layer, the net flux is assessed accounting for the following main terms

$$H_{\text{net}} = H_{\text{s}} + H_{\text{a}} + H_{\text{w}} + H_{\text{e}} + H_{\text{c}} + H_{\text{p}} + H_{\text{i}} + H_{\text{d}}, \tag{A1}$$

where H_{s} is the net short-wave radiative heat flux due to solar radiation (considering only the incoming radiation that is actually absorbed), H_{a} is the net long-wave radiation emitted from the atmosphere toward the lake, H_{w} is the long-wave radiation emitted from the water, H_{e} is the latent heat flux (due to evaporation/condensation processes), H_{c} is the sensible heat flux (due to convection), H_{p} is the heat flux due to precipitation onto the water surface, H_{i} is the effect of the throughflow of water by inlets and outlets, and H_{d} is the heat flux exchanged with deep water. Figure 1 shows a schematic representation of the heat exchanges at the epilimnion/atmosphere and epilimnion/hypolimnion interfaces. All the components of Eq. (A1) are analyzed in detail below to point out the main variables and physical parameters involved in the heat exchange process.

The incident short-wave solar radiation approximately follows a sinusoidal annual cycle. Considering the short-wave reflectivity r_{s} (albedo), which is a function of the solar zenith angle and of the lake surface conditions (e.g. water waves height), the net solar radiation H_{s} reads

$$H_{\text{s}} = (1 - r_{\text{s}}) \left[s_1 \cos\left(\frac{2\pi\,(t - s_2)}{t_{\text{y}}} \right) + s_3 \right], \tag{A2}$$

Discussion Paper | Discussion Paper | Discussion Paper | Discussion Paper |

where t is time, t_y is the duration of a year in the units of time considered in the analysis, and s_1, s_2, s_3 are coefficients that primarily depends on the latitude and the shadowing effects of the local topography. The effects of cloud cover, which could be accounted for by means of empirical relationships, are not explicitly considered in the present analysis.

Long-wave radiation terms are calculated according to the Stefan-Boltzmann law, yielding to the following formulations

$$H_\mathrm{a} = (1 - r_\mathrm{a})\epsilon_\mathrm{a}\sigma\left(T_\mathrm{K} + T_\mathrm{a}\right)^4, \tag{A3}$$

$$H_\mathrm{w} = -\epsilon_\mathrm{w}\sigma\left(T_\mathrm{K} + T_\mathrm{w}\right)^4, \tag{A4}$$

where r_a is the long wave reflectivity, generally assumed to have a constant values (Henderson-Sellers, 1986), ϵ_a and ϵ_w are the emissivities of atmosphere and lake surface, respectively, σ is the Stefan–Boltzmann constant ($5.67 \times 10^{-8}\,\mathrm{W\,m^{-2}\,K^{-4}}$), $T_\mathrm{K} = 273.15\,\mathrm{K}$, T_a and T_w are the temperatures of air and water expressed in Celsius [°C]. The emissivity ϵ_w is essentially constant and close to unity, as water is nearly a black body, while ϵ_a is more variable and depends on several factors among which the most important are air temperature, humidity and cloud cover (Imboden and Wüest, 1995).

Air and water temperatures can be decomposed into a reference value representative of the specific case study ($\overline{T_\mathrm{a}}$ and $\overline{T_\mathrm{w}}$) and a fluctuation (T'_a and T'_w). Hence, considering that $T'_\mathrm{a}/(T_\mathrm{K} + \overline{T_\mathrm{a}})$ and $T'_\mathrm{w}/(T_\mathrm{K} + \overline{T_\mathrm{w}})$ are small parameters, the long-wave fluxes Eqs. (A3) and (A4) can be linearised using a Taylor expansion as

$$H_\mathrm{a} \simeq \tilde{\epsilon}_\mathrm{a}\sigma\left(T_\mathrm{K} + \overline{T_\mathrm{a}}\right)^4\left(1 + 4\frac{T'_\mathrm{a}}{T_\mathrm{K} + \overline{T_\mathrm{a}}}\right), \tag{A5}$$

$$H_\mathrm{w} \simeq -\epsilon_\mathrm{w}\sigma\left(T_\mathrm{K} + \overline{T_\mathrm{w}}\right)^4\left(1 + 4\frac{T'_\mathrm{w}}{T_\mathrm{K} + \overline{T_\mathrm{w}}}\right), \tag{A6}$$

where $\tilde{\epsilon}_\mathrm{a} = (1 - r_\mathrm{a})\epsilon_\mathrm{a}$. By choosing $\overline{T_\mathrm{a}} = \overline{T_\mathrm{w}} = \overline{T}$ (hence $T'_\mathrm{a} = T_\mathrm{a} - \overline{T}$ and $T'_\mathrm{w} = T_\mathrm{w} - \overline{T}$), the terms H_a and H_w can be easily combined to yield the following equation

$$H_\mathrm{a} + H_\mathrm{w} \simeq 4\sigma\tilde{\epsilon}_\mathrm{a}\left(T_\mathrm{K} + \overline{T}\right)^3 \cdot \left[\frac{\tilde{\epsilon}_\mathrm{a} - \epsilon_\mathrm{w}}{4\tilde{\epsilon}_\mathrm{a}}\left(T_\mathrm{K} + \overline{T}\right) + \frac{\tilde{\epsilon}_\mathrm{a} - \epsilon_\mathrm{w}}{\tilde{\epsilon}_\mathrm{a}}\left(T_\mathrm{w} - \overline{T}\right) + T_\mathrm{a} - T_\mathrm{w}\right]. \tag{A7}$$

Discussion Paper | Discussion Paper | Discussion Paper | Discussion Paper |

The sensible (H_c) and latent (H_e) heat fluxes are calculated through bulk semi-empirical relations that can be derived from turbulence theory (Henderson-Sellers, 1986)

$$H_\mathrm{c} = \alpha_c \left(T_\mathrm{a} - T_\mathrm{w}\right), \tag{A8}$$
$$H_\mathrm{e} = \alpha_e \left(e_\mathrm{a} - e_\mathrm{w}\right), \tag{A9}$$

where α_c [W m^{-2} K^{-1}] and α_e [W m^{-2} hPa^{-1}] are transfer functions primarily depending on wind speed and other meteorological parameters, e_a is the vapor pressure in the atmosphere and e_w is the water vapor saturation pressure at the water temperature (both in [hPa]). The ratio α_c/α_e is known as Bowen coefficient and is often taken to be constant (≈ 0.61 hPa K^{-1}) (Imboden and Wüest, 1995). The saturated water pressure e_w is a function of temperature, and can be calculated through several empirical formulas, as for example the exponential law

$$e_\mathrm{w} = a \exp\left(\frac{bT_\mathrm{w}}{c + T_\mathrm{w}}\right), \tag{A10}$$

where $a = 6.112$ hPa, $b = 17.67$ and $c = 243.5$ °C (Bolton, 1980).

In order to keep the formulation of the model as simple as possible, Eq. (A10) can be linearized by Taylor series expansion around a reference temperature~~, which can be assumed equal to~~ $\overline{T}$

$$e_\mathrm{w} \approx a \exp\left(\frac{b\overline{T}}{\overline{T} + c}\right)\left(1 + \frac{bc}{\left(\overline{T} + c\right)^2}\left(T_\mathrm{w} - \overline{T}\right)\right). \tag{A11}$$

Finally, the heat exchange with deep water H_d can be formulated, as a first approximation, as the combination of a constant contribution and a contribution depending on the gradient of temperature between surface and hypolimnetic water. Considering that deep water has a temperature that is approximately constant during the year, the second component of H_d is essentially dependent on surface water temperature T_w. The term H_d is usually small with respect to the flux components exchanged with the atmosphere, which have been described above. Analogously, the contribution H_p of precipitation onto the lake surface and the heat H_i exchanged with the inflows and the outflows are only rarely significant, thus are not explicitly included in the balance. As a matter of fact, changes in surface temperature during rainy periods

Discussion Paper | Discussion Paper | Discussion Paper | Discussion Paper |

generally result from changes of the main terms H_{w}, H_{c} and H_{e}, and H_{i} is only important in lakes with high flushing rate (Imboden and Wüest, 1995).

Under these hypotheses, and adopting the heat flux terms provided above, the net heat flux at the surface H_{net} introduced in Eq. (A1) can be suitably written as the combination of the linear and sinusoidal functions in Eq. (1), where c_i (i from 1 to 5) are coefficients resulting by appropriately combining together the physical parameters that appear in Eqs. (A2)–(A11).

By assuming the parameters inherently influenced by meteorological (e.g. wind, cloudiness and precipitation ~~patterns~~) and astronomical phenomena (i.e. r_{s}, α_c, α_e, e_{a}) as the combination of a mean (indicated by an overline) and a periodic (indicated by a prime) component, the coefficients c_i can be expressed as follows

$$c_1 \approx (1-\overline{r}_{\mathrm{s}})\, s_1 + f\left(r'_{\mathrm{s}},\, \alpha'_c,\, \alpha'_e,\, e'_{\mathrm{a}}\right), \tag{A12}$$

$$c_2 \in [0,\, 1], \tag{A13}$$

$$c_3 \approx (1-\overline{r}_{\mathrm{s}})\, s_3 + \sigma\left(\tilde{\epsilon_{\mathrm{a}}} - \epsilon_{\mathrm{w}}\right)\left(T_{\mathrm{K}}+\overline{T}\right)^3\left(T_{\mathrm{K}}-3\overline{T}\right) - \overline{\alpha}_e\left[\overline{e}_{\mathrm{a}} - a\exp\left(\frac{b\overline{T}}{\overline{T}+c}\right)\left(1-\frac{bc}{\left(\overline{T}+c\right)^2}\overline{T}\right)\right], \tag{A14}$$

$$c_4 \approx 4\sigma\tilde{\epsilon_{\mathrm{a}}}\left(T_{\mathrm{K}}+\overline{T}\right)^3 + \overline{\alpha}_{\mathrm{c}}, \tag{A15}$$

$$c_5 \approx 4\sigma\left(T_{\mathrm{K}}+\overline{T}\right)^3\left(\tilde{\epsilon_{\mathrm{a}}} - \epsilon_{\mathrm{w}}\right) - \overline{\alpha}_e\, a\exp\left(\frac{b\overline{T}}{\overline{T}+c}\right)\left(\frac{bc}{\left(\overline{T}+c\right)^2}\right). \tag{A16}$$

~~It is worth noting that a~~ A straightforward quantification of this set of coefficients is not trivial. In fact, most of the physical parameters involved do not have a single, unambiguous value, but rather they span a range of values that depends on several factors that are difficult to specify (e.g. cloud cover).

As a final remark, it is worth ~~to note~~ noting that the first term on the right hand side of Eq. (1) is a periodic term accounting for all seasonal patterns of meteorological variables other than air temperature (e.g. wind speed, air humidity, cloudiness, see the definition of c_1). As a first approximation, these components have been treated as sinusoidal functions having the same frequency of the solar radiation (i.e. a period equal to one year), but possibly different amplitudes and phases. The sum of such a set of functions produces another sinusoid having the same frequency but different amplitude, c_1, and phase, c_2.

Discussion Paper | Discussion Paper | Discussion Paper | Discussion Paper |

Acknowledgements. The authors are grateful to the NOAA (National Oceanic and Atmospheric Administration) for providing the data used in this work. We thank Martin Schmid for a careful reading of a preliminary version of the manuscript. We also acknowledge Masataka Okabe and Kei Ito for the helpful guideline on how to make colorblind-friendly figures, which we followed for producing the plots (web link: jfly.iam.u-tokyo.ac.jp/html/color_blind).

References

Adrian, R., O'Reilly, C. M., Zagarese, H., Baines, S. B., Hessen, D. O., Keller, W., Livingstone, D. M., Sommaruga, R., Straile, D., Donk, E. V., Weyhenmeyer, G. A., and Winder, M.: Lakes as sentinels of climate change, Limnology and Oceanography, 54, 2283–2297, 2009.

Arhonditsis, G. B., Brett, M. T., DeGasperi, C. L., and Schindler, D. E.: Effects of climatic variability on the thermal properties of Lake Washington, Limnology and Oceanography, 49, 256–270, 2004.

Benyahya, L., Cassie, F., St-Hilaire, A., Ourada, T. B., and Bobe, B.: A Review of Statistical Water Temoerature Models, Canadian Water Resources Journal, 32, 179–192, 2007.

Beven, K. J.: A manifesto for the equifinality thesis, Water Resources Research, 320, 18–36, 2006.

Beven, K. J. and Binley, A. M.: The future of distributed models: Model calibration and uncertainty prediction, Hydrological Processes, 6, 279–288, 1992.

Bilello, M. A.: Method for predicting river and lake ice formation, Journal of Applied Meteorology, 3, 38–44, 1964.

Bolton, D.: The Computation of Equivalent Potential Temperature, Monthly Weather Review, 108, 1046–1053, 1980.

Butcher, J. C.: Numerical Methods for Ordinary Differential Equations, John Wiley & Sons Inc, 2003.

Crisp, D. T. and Howson, G.: Effect of Air Temperature upon Mean Water Temperature in Streams in the North Pennines and English Lake District, Freshwater Biology, 12, 359–367, 1982.

Fang, X. and Stefan, H. G.: Long-term lake water temperature and ice cover simulations/measurements, Cold Regions Science and Technology, 24, 289–304, 1996.

Fang, X. and Stefan, H. G.: Projections of climate change effects on water temperature characteristics of small lakes in the contiguous U.S., Climatic Change, 42, 377–412, 1999.

Gleckler, P. J., Taylor, K. E., and Doutriaux, C.: Performance metrics for climate models, Journal of Geophysical Research, 113, D06 104, 2008.

Goudsmit, G. H., Burchard, H., Peeters, F., and Wüest, A.: Application of k-ϵ turbulence models to

enclosed basins: The role of internal seiches, Journal of Geophysical Research: Oceans, 107, 23–1–23–13, 2002.

Goyette, S. and Perroud, M.: Interfacing a one-dimensional lake model with a single-column atmospheric model: Application to the deep Lake Geneva, Switzerland, Water Resources and Research, 48, W04 507, 2012.

Henderson-Sellers, B.: Calculating the surface energy balance for lake and reservoir modeling: A review, Reviews of Geophysics, 24, 625–649, 1986.

Hornberger, G. M., Beven, K. J., Cosby, B. J., and Sappington, D. E.: Shenandoah watershed study: calibration of a topography-based, variable contributing area hydrological model to a small forested catchment, Water Resources and Research, 21, 1841–1850, 1985.

Hutchinson, G. E. and Löffler, H.: The thermal classification of lakes, Proceedings of the National Academy of Sciences of the United States of America, 42, 84–86, 1956.

Imboden, D. M. and Wüest, A.: Physics and Chemistry of Lakes, chap. 4 Mixing Mechanisms in Lakes, pp. 83–138, Springer-Verlag, 1995.

Kettle, H., Anderson, R. T. N. J., and Livingstone, D. M.: Empirical modeling of summer lake surface temperatures in southwest Greenland, Limnology and Oceanography, 49, 271–282, 2004.

Kothandaraman, V. and Evans, R. L.: Use of Air-Water Relationships for Predicting Water Temperature, Tech. rep., Illinois State Water Survey, Urbana, report of Investigation 69, 1972.

Lewis, W. M.: A Revised Classification of Lakes Based on Mixing, Canadian Journal of Fisheries and Aquatic Sciences, 40, 1779–1787, 1983.

Livingstone, D. M. and Lotter, A. F.: The relationship between air and water temperatures in lakes of the Swiss Plateau: a case study with palæolimnological implications, Journal of Paleolimnology, 19, 181–198, 1998.

Livingstone, D. M. and Padisák, J.: Large-scale coherence in the response of lake surface-water temperatures to synoptic-scale climate forcing during summer, Limnology and Oceanography, 52, 896–902, 2007.

Livingstone, D. M., Lotter, A. F., and Ian, R. W.: The Decrease in Summer Surface Water Temperature with Altitude in Swiss Alpine Lakes: A Comparison with Air Temperature Lapse Rates, Arctic, Antarctic, and Alpine Research, 31, 341–352, 1999.

MacKay, M. D., Neale, P. J., Arp, C. D., Domis, L. N. D. S., Fang, X., Gal, G., Joehnk, K. D., Kirillin, G., Lenters, J. D., Litchman, E., MacIntyre, S., Marsh, P., Melack, J., Mooij, W. M., Peeters, F., Quesada, A., Schladow, S. G., Schmid, M., Spence, C., and Stokes, S. L.: Modeling lakes and reservoirs in the climate system, Limnology and oceanography, 54, 2315–2329, 2009.

Majone, B., Bertagnoli, A., and Bellin, A.: A non-linear runoff generation model in small Alpine catchments, Journal of Hydrology, 385, 300–312, 2010.

Majone, B., Bovolo, C. I., Bellin, A., Blenkinsop, S., and Fowler, H. J.: Modeling the impacts of future climate change on water resources for the Gàllego river basin (Spain), Water Resources and Research, 48, W01 512, 2012.

Martin, J. L. and McCutcheon, S.: Hydrodynamics and Transport for Water Quality Modeling, CRC Press, 1998.

Martynov, A., Sushama, L., and Laprise, R.: Simulation of temperate freezing lakes by one-dimensional lake models: performance assessment for interactive coupling with regional climate models, Boreal Environment Research, 15, 143–164, 2010.

Martynov, A., Sushama, L., Laprise, R., Winger, K., and Dugas, B.: Interactive lakes in the Canadian Regional Climate Model, version 5: the role of lakes in the regional climate of North America, Tellus A, 64, 2012.

McCombie, A. M.: Some Relations Between Air Temperatures and the Surface Water Temperatures of Lakes, Limnology and Oceanography, 4, 252–258, 1959.

Morrill, J. C., Bales, R. C., and Conklin, M.: Estimating Stream Temperature from Air Temperature: Implications for Future Water Quality, Journal of Environmental Engineering, 131, 139–146, 2005.

Nash, J. E. and Sutcliffe, J. V.: River flow forecasting through conceptual models 1. A discussion of principles, Journal of Hydrology, 10, 282–290, 1970.

Peeters, F., Livingstone, D. M., Goudsmit, G. H., Kipfer, R., and Forster, R.: Modeling 50 years of historical temperature profiles in a large central European lake, Limnology and Oceanography, 47, 186–197, 2002.

Piccolroaz, S.: Deep ventilation in Lake Baikal: a simplified model for a complex natural phenomenon, Ph.D. thesis, Doctoral School in Environmental Engineering, University of Trento (Italy), 2013.

Piccolroaz, S. and Toffolon, M.: Deep ventilation in Lake Baikal: a model for long term analyses, submitted to Journal of Geophysical Research, 2013.

Rodhe, B.: On the Relation between Air Temperature and Ice Formation in the Baltic, Geografiska Annaler, 34, 175–202, 1952.

Schwab, B. J., Leshkevich, G. A., and Muhr, G. C.: Automated Mapping of Surface Water Temperature in the Great Lakes, Journal of Great Lakes Research, 25, 468–481, 1999.

Sharma, S., Walker, S. C., and Jackson, D. A.: Empirical modelling of lake water-temperature relationships: a comparison of approaches, Freshwater Biology, 53, 897–911, 2008.

Shuter, B. J., Schlesinger, D. A., and Zimmerman, A. P.: Empirical Predictors of Annual Surface Water

Temperature Cycle in North American Lakes, Canadian Journal of Fisheries and Aquatic Sciences, 40, 1838–1845, 1983.

Stefan, H. G., Fang, X., and Hondzo, M.: Simulated climate change effects on year-round water temperatures in temperate zone lakes, Climatic Change, 40, 547–576, 1998.

Webb, M. S.: Surface Temperatures of Lake Erie, Water Resources Research, 10, 199–210, 1974.

Webb, M. S., Clack, P. D., and Walling, D. E.: Water-air temperature relationships in a Devon river system and the role of flow, Water Resources Research, 17, 3069–3084, 2003.

Wetzel, R. G.: Limnology: Lake and River Ecosystems, Academic Press, San Diego, 3 edn., 2001.

Discussion Paper | Discussion Paper | Discussion Paper | Discussion Paper |

Table 1. Summary of the datasets adopted in this study, and their main statistics.

Source	Variable	Device	Period	Duration (cal + val)	Frequency	Missing data	Mean value [$^{\circ}C$]	Std [$^{\circ}C$]
NDBC	T_w	Offshore buoy	1985-2011	27 years (18 + 9)	Hourly	46%	7.18	4.66
NDBC	T_a	C-MAN station	1985-2011	27 years (18 + 9)	Hourly	9%	5.39	8.97
GLERL	T_w	Satellite	1994-2011	18 years (12 + 6)	Daily	5%	6.52	5.26

Table 2. Estimated model parameters for NDBC, GLERL and GLERL$_{my}$ simulations, and their physical range of variation.

n par.	p_1 [$^{\circ}C\ d^{-1}$]	p_2 [$-$]	p_3 [$^{\circ}C\ d^{-1}$]	p_4 [d^{-1}]	p_5 [d^{-1}]	p_6 [$^{\circ}C$]	p_7 [$^{\circ}C$]	p_8 [$^{\circ}C$]
min	0.00	0.00	-0.12	0.00	-0.02	0	0	0
max	0.33	1.00	0.28	0.01	-0.00	15	15	0.5
				NDBC				
8	1.35x10^{-2}	2.62x10^{-1}	1.47x10^{-3}	6.18x10^{-3}	-3.26x10^{-4}	3.08	14.41	0.31
6	1.56x10^{-2}	2.83x10^{-1}	1.23x10^{-3}	5.95x10^{-3}	-2.36x10^{-4}	3.01	-	-
4	-	-	1.41x10^{-2}	5.87x10^{-3}	-2.23x10^{-3}	2.77	-	-
				GLERL				
8	1.75x10^{-2}	4.67x10^{-1}	2.30x10^{-2}	6.55x10^{-3}	-2.57x10^{-3}	3.50	13.32	0.44
6	2.36x10^{-2}	4.37x10^{-1}	1.93x10^{-2}	5.91x10^{-3}	-2.16x10^{-3}	3.65	-	
4	-	-	2.57x10^{-2}	9.63x10^{-3}	-2.73x10^{-3}	3.54	-	-
				GLERL$_{my}$				
8	1.31x10^{-2}	2.32x10^{-1}	1.55x10^{-2}	8.47x10^{-3}	-1.09x10^{-3}	3.26	11.93	0.45
6	2.01x10^{-2}	2.06x10^{-1}	1.49x10^{-2}	9.69x10^{-3}	-7.58x10^{-4}	3.75	-	-
4	-	-	2.77x10^{-2}	9.16x10^{-3}	-2.87x10^{-3}	3.13	-	-

Discussion Paper | Discussion Paper | Discussion Paper | Discussion Paper |

Table 3. Efficiency index (E), Root Mean Square Error ($RMSE$) and Mean Error (ME) during calibration and validation periods (NDBC, GLERL and GLERL$_{my}$ simulations).

	calibration			validation		
n par.	E [–]	$RMSE$ [°C]	ME [°C]	E [–]	$RMSE$ [°C]	ME [°C]
NDBC (cal: 1985-2002; val: 2003-2011)						
8	0.91	1.40	-0.07	0.90	1.71	-0.01
6	0.91	1.35	-0.09	0.90	1.71	-0.02
4	0.89	1.50	-0.25	0.89	1.77	-0.01
GLERL (cal: 1994-2005; val: 2006-2011)						
8	0.95	1.17	-0.13	0.97	1.02	0.30
6	0.95	1.16	-0.07	0.97	1.01	0.33
4	0.95	1.21	-0.05	0.97	1.08	0.38
GLERL$_{my}$ (cal: mean year 1994-2005; val: 2006-2011)						
8	0.99	0.48	0.06	0.97	1.07	0.23
6	0.99	0.43	0.01	0.97	0.98	0.15
4	0.99	0.47	0.03	0.97	1.11	0.29

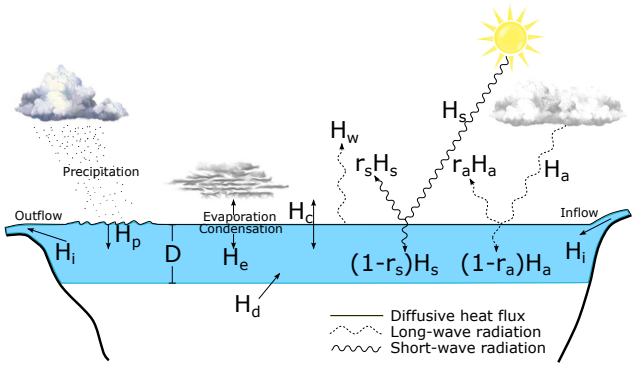

Fig. 1. Main heat exchange affecting the surface layer. For the description of the single terms refer to Appendix A.

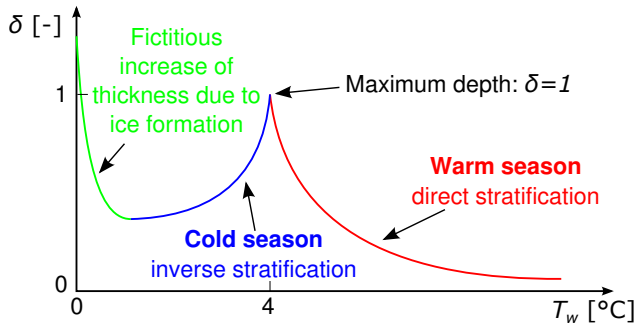

Fig. 2. Seasonal evolution of the dimensionless thickness δ of the surface well-mixed layer for the general case of a dimictic lake.

Discussion Paper | Discussion Paper | Discussion Paper | Discussion Paper |

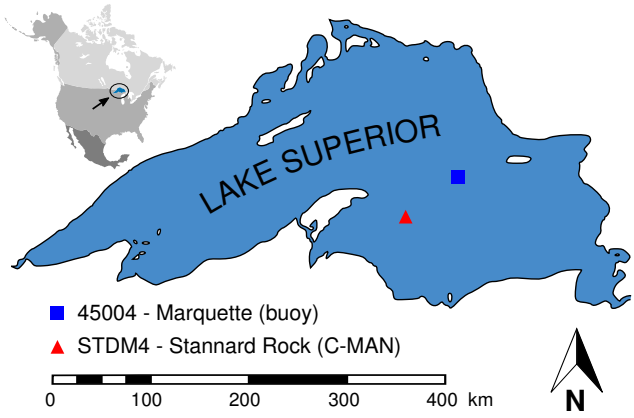

Fig. 3. Lake Superior with the location of the NDBC stations (45004 - Marquette and STDM4 - Stannard Rock) used in this work. The inset shows the location of lake Superior in North America.

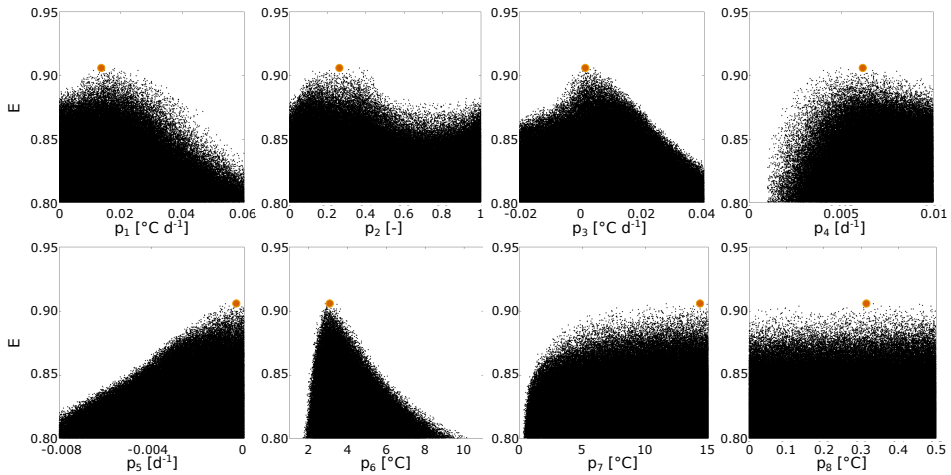

Fig. 4. Dotty plots of efficiency indexes (E) for the 8-parameters model during the calibration period 1985-2002 (NDBC simulation). Highest efficiency is presented with an orange dot.

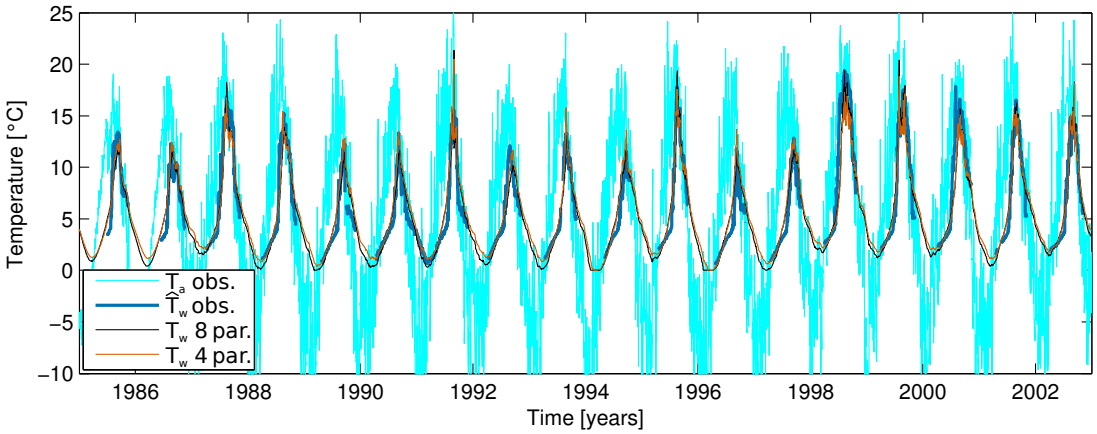

Fig. 5. Comparison between simulated and observed surface water temperature during the calibration period 1985-2002 (NDBC simulation). Simulated curves refer to the full 8-parameter and the simplified 4-parameter models, respectively. Observed air temperature data are also presented with cyan line.

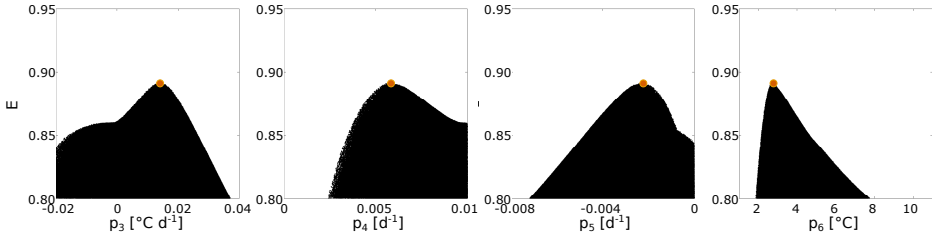

Fig. 6. Dotty plots of efficiency indexes (E) for the 4-parameters model during the calibration period 1985-2002 (NDBC simulation). Highest efficiency is presented with an orange dot.

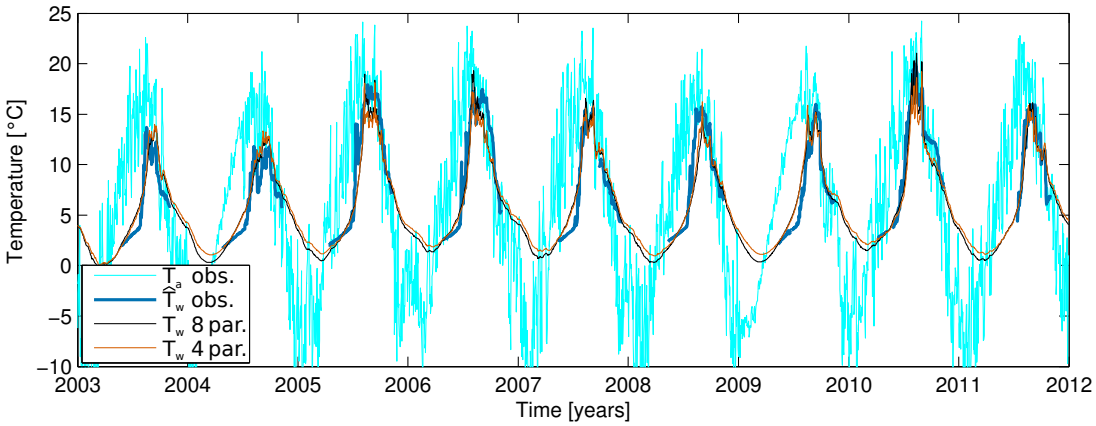

Fig. 7. Comparison between simulated and observed surface water temperature during the validation period 2003-2011 (NDBC simulation). Simulated curves refer to the full 8-parameter and the simplified 4-parameter models, respectively. Observed air temperature data are also presented with cyan line.

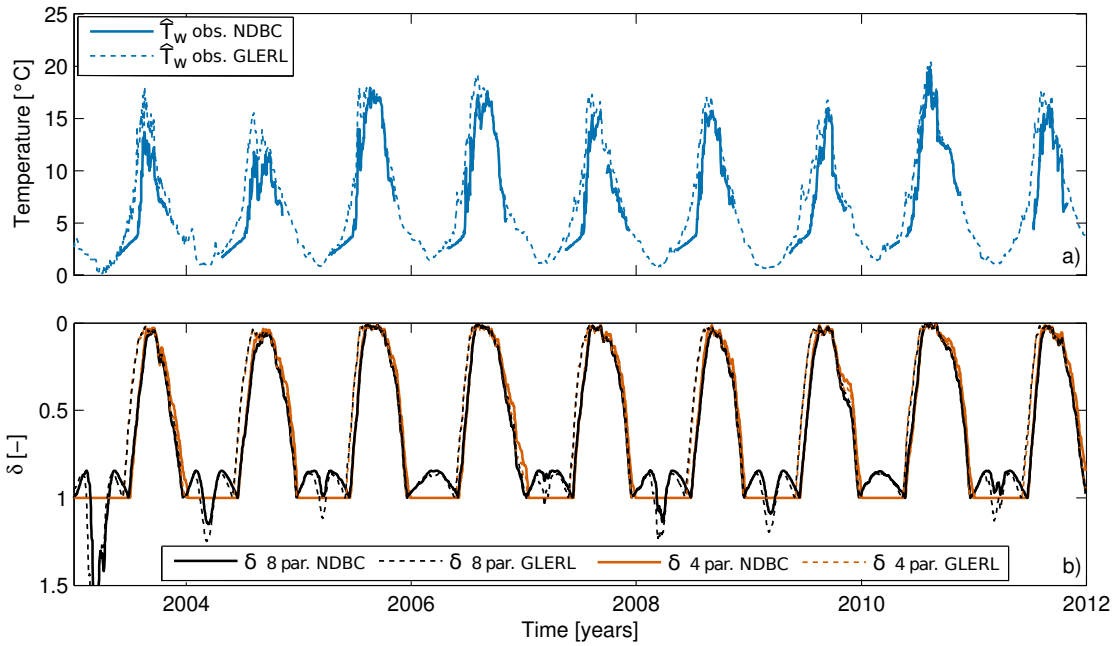

Fig. 8. Evolution of the dimensionless depth δ over the period 2003-2011: comparison between results for the full 8- and simplified 4-parameter versions of the model obtained from NDBC and GLERL simulations. a) Comparison of observed water temperature time series during the period 2003-2011 for the NDBC and GLERL dataset, respectively. b) Evolution of the dimensionless depth δ over the period 2003-2011 for the full 8- and simplified 4-parameter versions of the model (NDBC and GLERL simulations).

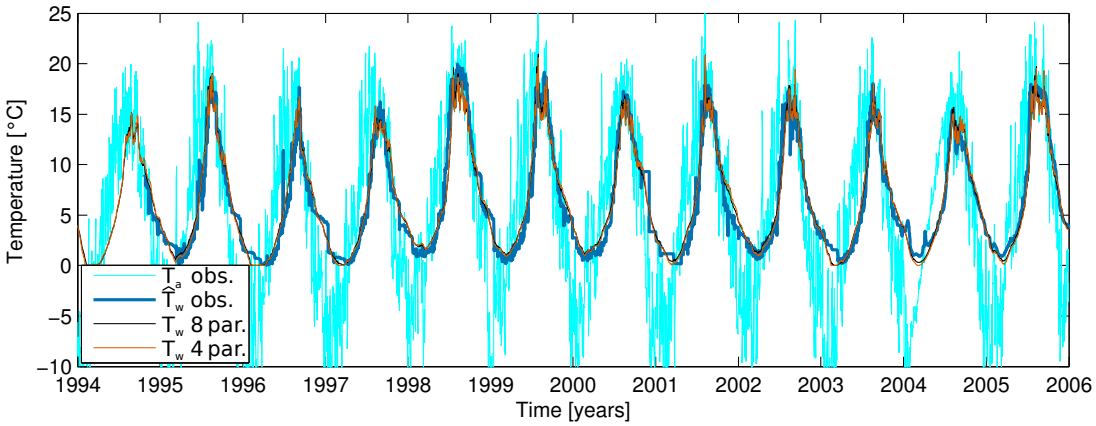

Fig. 9. Comparison between simulated and observed surface water temperature during the calibration period 1994-2005 (GLERL simulation). Simulated curves refer to the full 8-parameter and the simplified 4-parameter models, respectively. Observed air temperature data are also presented with cyan line.

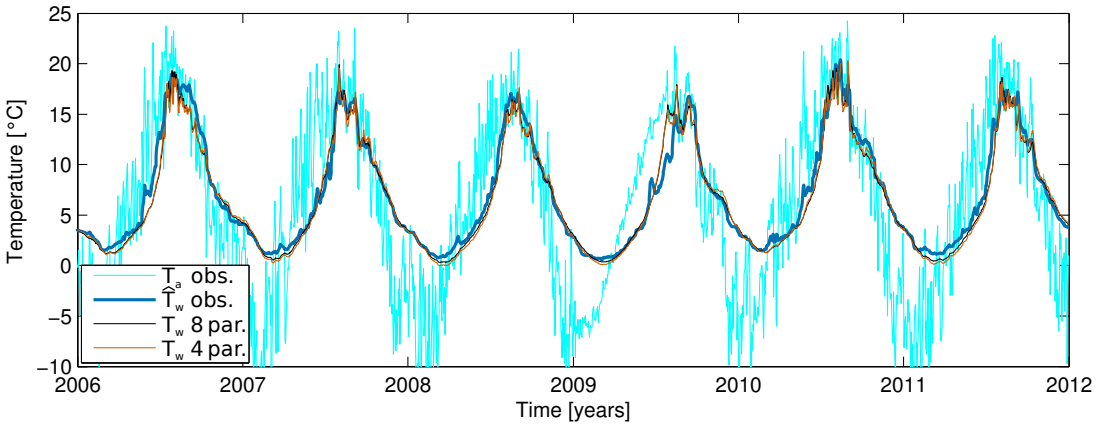

Fig. 10. Comparison between simulated and observed surface water temperature during the validation period 2006-2011 (GLERL simulation). Simulated curves refer to the full 8-parameter and the simplified 4-parameter models, respectively. Observed air temperature data are also presented with cyan line.

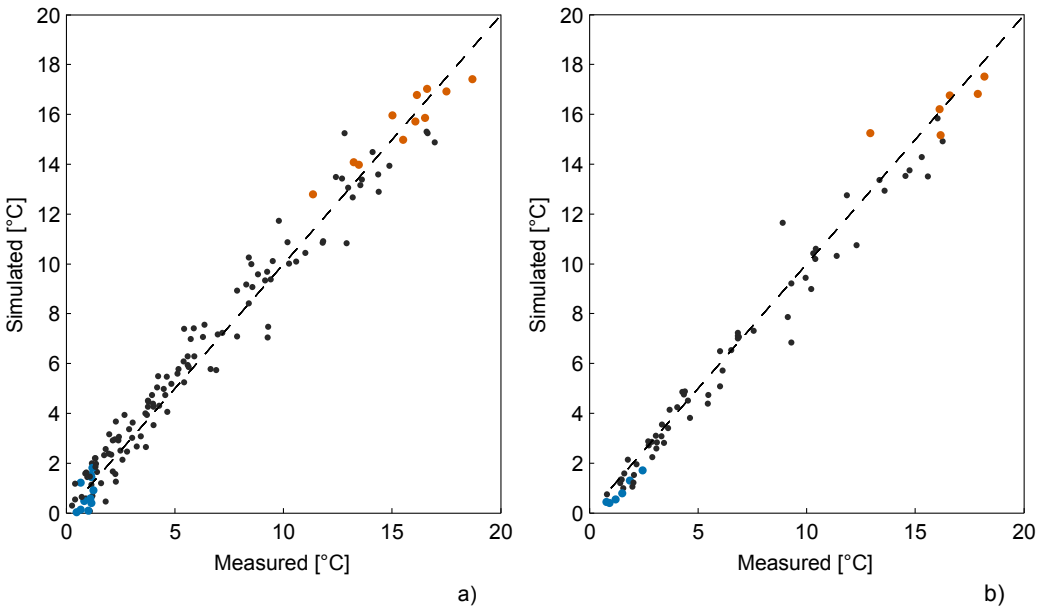

Fig. 11. Parity diagram for monthly-averaged surface water temperature (8-parameters version of the model): a) calibration and b) validation period of the GLERL simulation. Blue dots refer to March, red dots to August and grey dots to the remaining months of the year.

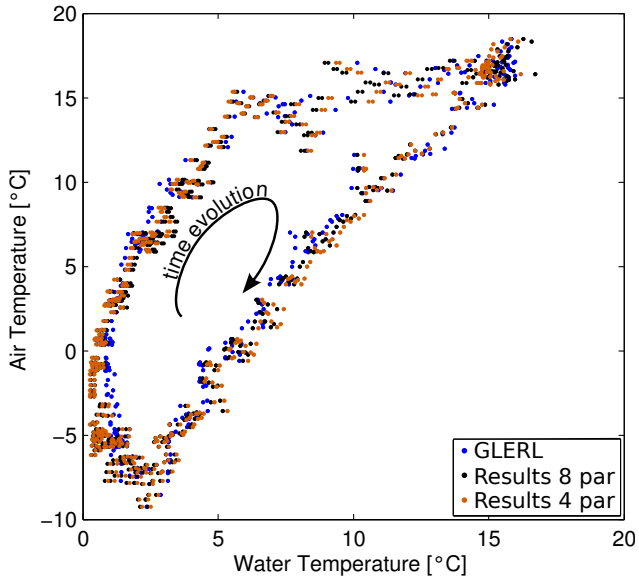

Fig. 12. Comparison of the hysteresis cycles between daily air and surface water temperatures, as derived by the data and by the 8- and 4-parameters versions of the model. Hysteresis cycles refer to the mean year, calculated over the period 1994-2005, using GLERL and NDBC data for T_w and T_a, respectively (GLERL$_{my}$ simulation).